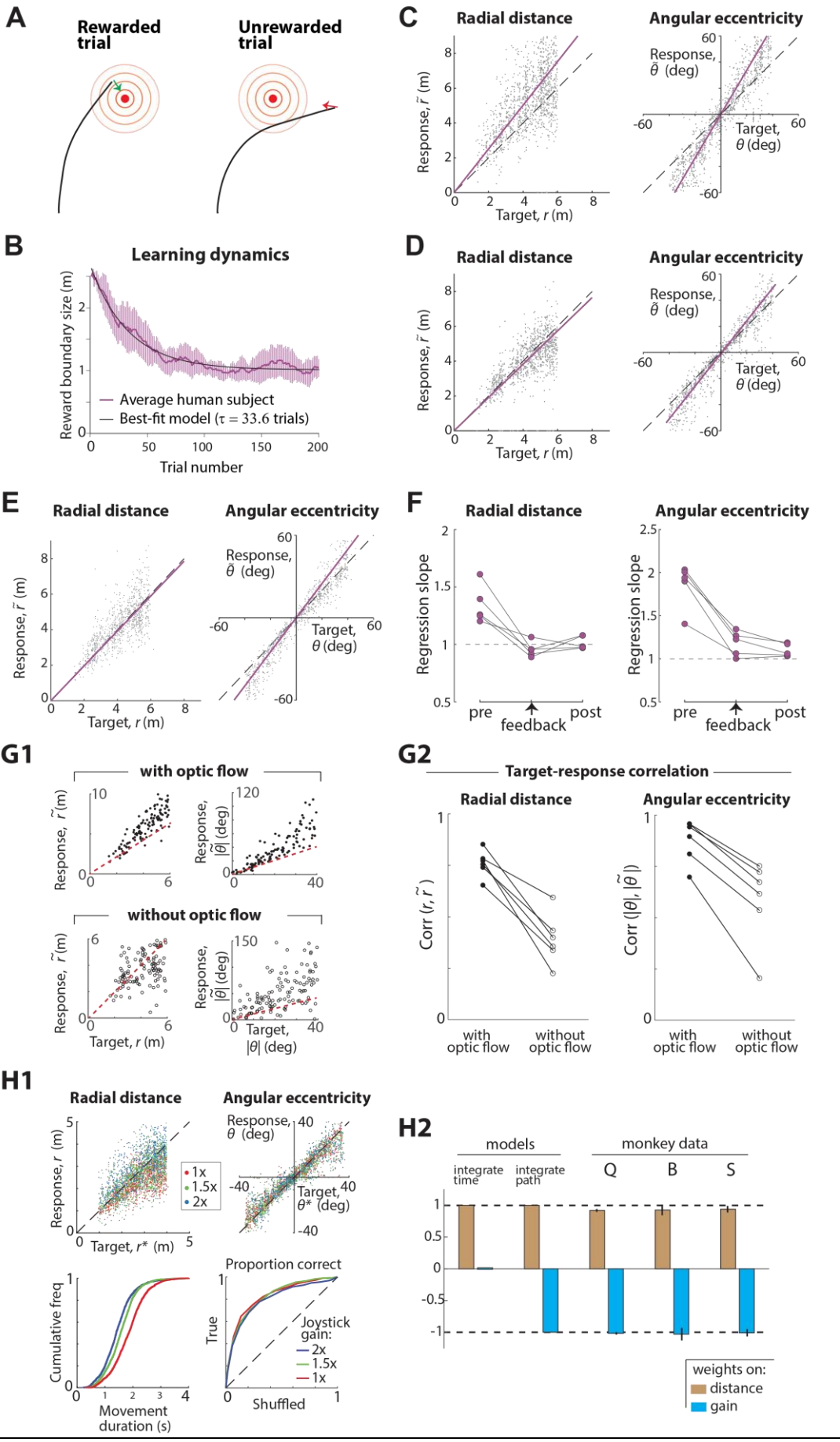
A
Rewarded trial
Unrewarded trial
B
Learning dynamics
Reward boundary size (m)
Average human subject
Best-fit model (τ = 33.6 trials)
Trial number
C
Radial distance
Angular eccentricity
Response, r̃ (m)
Target, r (m)
Response, θ̃ (deg)
Target, θ (deg)
D
Radial distance
Angular eccentricity
E
Radial distance
Angular eccentricity
F
Radial distance
Angular eccentricity
Regression slope
pre
feedback
post
G1
with optic flow
without optic flow
Response, r̃ (m)
Response, |θ̃| (deg)
Target, r (m)
Target, |θ| (deg)
G2
Target-response correlation
Radial distance
Angular eccentricity
Corr (r, r̃)
Corr (|θ|, |θ̃|)
with optic flow
without optic flow
H1
Radial distance
Angular eccentricity
Response, r (m)
Target, r* (m)
Response, θ (deg)
Target, θ* (deg)
1x
1.5x
2x
Cumulative freq
Movement duration (s)
Proportion correct
True
Shuffled
Joystick gain:
2x
1.5x
1x
H2
models
monkey data
integrate time
integrate path
Q
B
S
weights on:
distance
gain

Figure S1. [Related to **Figure 1**] **A. Feedback for humans.** At the end of the movement, a bullseye pattern (concentric rings) centred on the target appeared on the ground plane to indicate the magnitude of error. The arrowhead served both as binary feedback (green – correct, red – incorrect) and to indicate the direction of error. **B. Learning rate.** The radius of the bullseye pattern was adaptively scaled using a staircase procedure (see **Methods**). Purple curve shows the average radius (R) across subjects as a function of trial number. Error bars denote ±1 standard deviation. The black curve shows the exponential function $R(n) \propto \exp(-n/\tau)$ fit to data. **C. Pre-feedback performance.** *Left*: Comparison of the radial distance of the response (final stopping position) against radial distance of the target across all trials of all human subjects during the first experimental block (pre-feedback block). *Right*: Angular eccentricity of subjects' response vs target angle. Black dashed lines have unity slope (unbiased performance). **D. Performance improved with feedback.** Similar to (C), but for the last 150 trials of the block with feedback (second block). **E. Performance improvement persisted after removing feedback.** Similar to (C), but for the final block of trials with feedback withheld (third block). **F.** Regression slopes of individual subjects across all three blocks (pre-feedback, feedback and post-feedback). **G. Human subjects rely on optic flow to perform the task.** [*Data from Lakshminarasimhan et al. (2018)*] Texture elements constituting the ground plane were removed in a random subset of trials to block optic flow cues. Subjects did not receive feedback at the end of the trials. (**G1**) Radial and angular response of an example human subject with (top panels) and without (bottom panels) optic flow cues. The subject's overall variability was much larger without optic flow cues. (**G2**) Across subjects, removing optic flow cues induced a significant decrease of target-response correlations in both radial distance [Corr(r,$\tilde{r}$) : 0.76±0.06 with optic flow, 0.39±0.12 without optic flow, p=4.1×10^{-4}, paired t-test] and angle [Corr($|\theta|$,$|\tilde{\theta}|$) : 0.88±0.1 with optic flow, 0.58±0.2 without optic flow, p=4.8×10^{-4}] suggesting that subjects relied heavily on optic flow cues. **H. Monkeys rely on optic flow to perform the task.** In separate blocks, we manipulated the gain of the joystick controller to alter the sensorimotor mapping learned by the monkey (gain values of 1x (baseline), 1.5x and 2x). Each block comprised around 500 trials and the order of the blocks were randomized across days. (**H1**) *Top panels*: Radial (*left*) and angular (*right*) response of an example monkey during trials from different gain conditions (red: 1x, green: 1.5x, blue:2x) showing that stopping positions were close to target locations under all conditions. *Bottom left*: Cumulative distribution of travel times for the different gain conditions. The mean travel time significantly decreased when gain was increased (mean ± std for 1x gain: 1.4±0.1s, 2x gain: 2.1±0.2s; $p < 10^{-5}$, paired t-test) implying that monkeys adapted to the different gain values by adjusting their travel duration appropriately. *Bottom right*: Average ROC curves of the monkeys, obtained by plotting their true proportion of correct trials (from unshuffled data) against the corresponding chance-level proportions (from shuffled data) for a range of reward windows separately for each gain condition. The area under the curve (AUC) was comparable under all three conditions (mean AUC ± std. for 1x gain: 0.82±0.03, 1.5x gain: 0.85±0.04, 2x gain: 0.79±0.06) implying that their task performance was not affected by manipulating the joystick gain . (**H2**) We simultaneously regressed the travel time against initial target distance (r) and joystick gain (g) in the log space across trials [$\log(T) = w_r \log(r) + w_g \log(g)$]. Travel time of an ideal path integrator would depend on changes in gain and have negative regression weight on the gain term ($w_g = -1$) whereas travel time for pure time integration or dead-reckoning would be insensitive to gain changes ($w_g = 0$). Across the set of all rewarded trials, the regression weight w_g on joystick gain was not significantly different from -1 in all three monkeys (95% confidence interval (CI) of regression weight, Monkey B: $[-0.99, -1.04]$, Monkey S: $[-0.95, -1.17]$, Monkey Q: $[-0.96, -1.09]$).

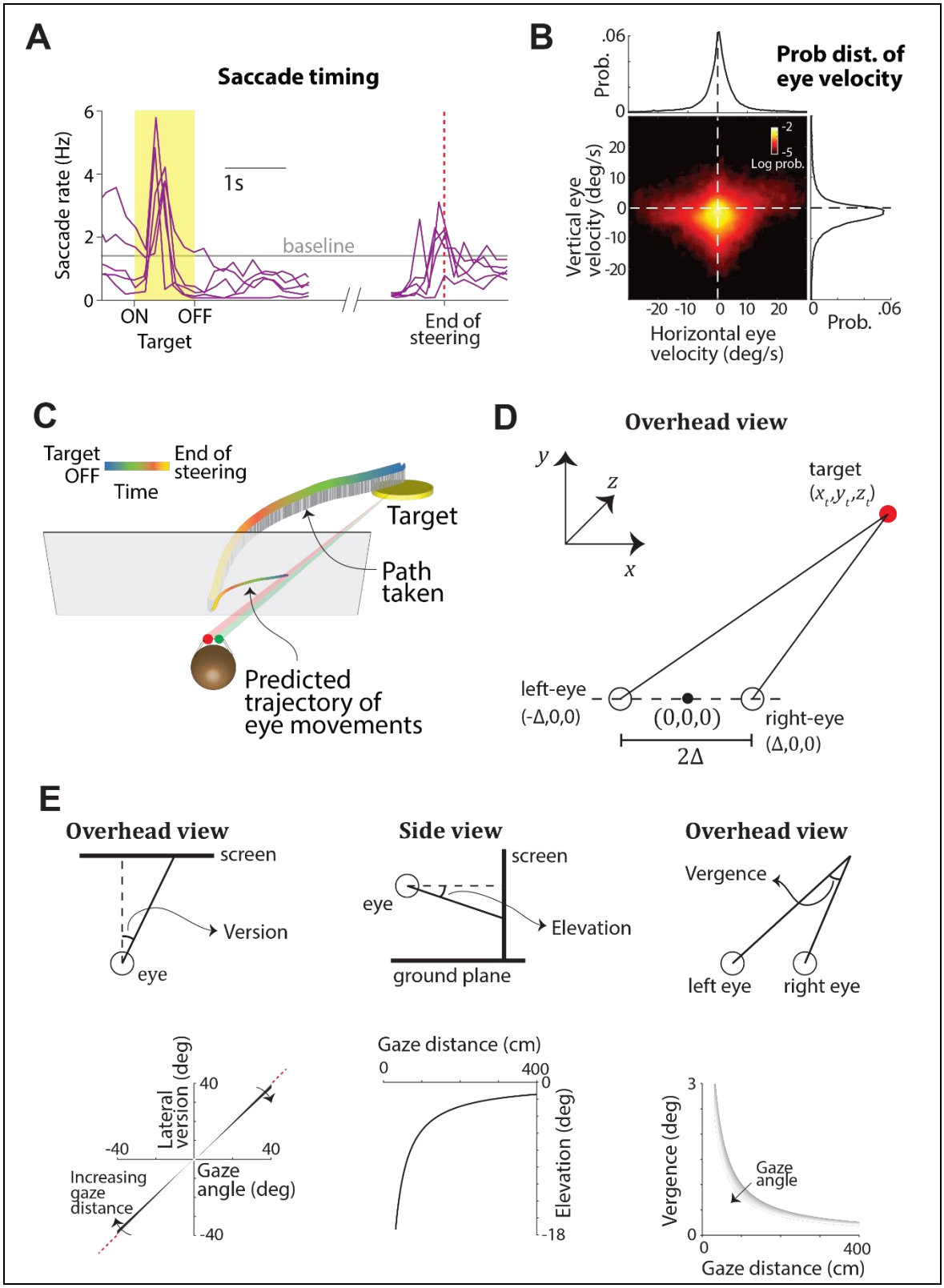
A
Saccade timing
Saccade rate (Hz)
6
4
2
0
1s
baseline
ON
OFF
Target
End of
steering
B
Prob dist. of
eye velocity
Prob.
.06
0
Vertical eye
velocity (deg/s)
20
10
0
-10
-20
-2
-5
Log prob.
-20 -10 0 10 20
Horizontal eye
velocity (deg/s)
0
Prob.
.06
C
Target
OFF
End of
steering
Time
Target
Path
taken
Predicted
trajectory of
eye movements
D
Overhead view
y
z
x
target
(x_t, y_t, z_t)
left-eye
(-Δ,0,0)
(0,0,0)
right-eye
(Δ,0,0)
2Δ
E
Overhead view
screen
Version
eye
Side view
screen
eye
Elevation
ground plane
Overhead view
Vergence
left eye
right eye
Lateral
version (deg)
40
-40
40
Increasing
gaze
distance
Gaze
angle (deg)
-40
Gaze distance (cm)
0
400
0
Elevation (deg)
-18
Vergence (deg)
3
Gaze
angle
0
0
400
Gaze distance (cm)

Figure S2. [Related to **Figure 2**]

Saccade timing and eye velocity of human subjects. A. The trial-averaged saccade rate of individual human subjects. Trials were aligned relative to target presentation (*shaded yellow* to the left of the break on the x-axis) and end of movement (*red dashed line* after the break). Note that targets were visible for a period of one second. **B.** The joint probability density of distribution over horizontal and vertical eye velocities, averaged across human subjects, while they steered towards the target.

Modelling angular eye position from 3d gaze location. C. Graphical illustration of the expected dynamics of subject's eye movements (average of the two eyes, projected onto the plane of the screen) while steering to the target. Time is coded by colour. **D.** The instantaneous three-dimensional egocentric position of the target (red) is used to generate theoretical predictions for the subject's eye position, assuming they maintained fixation at the centre of the target throughout the trial (**Methods – Equation 1**). **E.** *Top*: Eye position is characterized using three degrees of freedom: *Lateral version*, which measures the average deviation of the two eyes from the sagittal plane (*left*), *Elevation*, which measures the average deviation of the eyes from the transverse plane (*middle*), and *Vergence* which measures the difference between the lateral position of the two eyes (*right*, see **Methods** for quantitative definitions). *Bottom*: Theoretical dependence of the magnitudes of lateral version, elevation, and vergence on gaze distance and gaze angle (inter-ocular distance, $\Delta = 3.5$cm; eye height, $z = 10$cm).

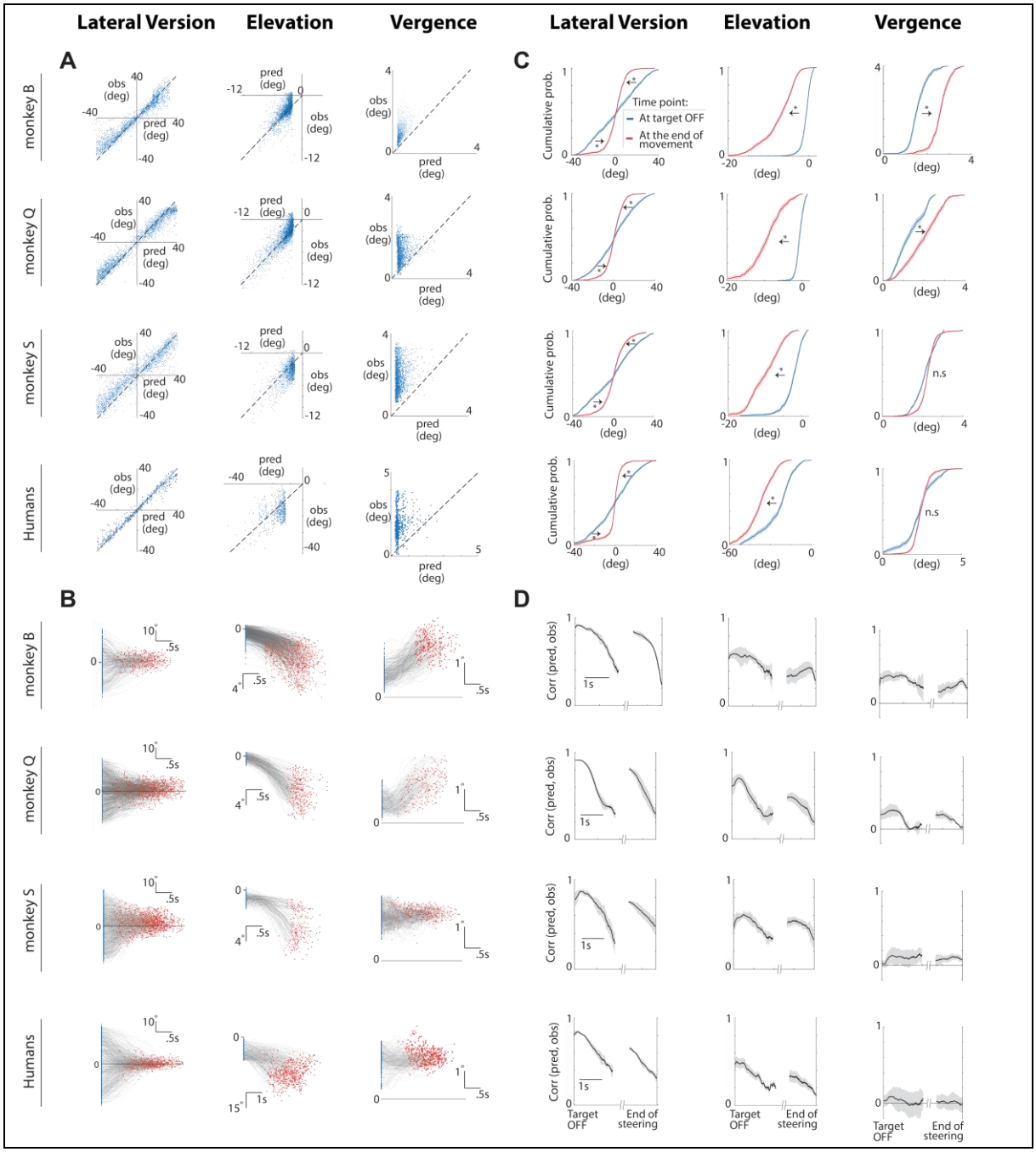
Lateral Version
Elevation
Vergence
Lateral Version
Elevation
Vergence
A
C
monkey B
monkey Q
monkey S
Humans
obs (deg)
pred (deg)
Cumulative prob.
Time point:
At target OFF
At the end of movement
(deg)
n.s
B
D
Corr (pred, obs)
1s
.5s
Target OFF
End of steering

Figure S3. [Related to **Figure 2**]

Temporal dynamics of lateral version, elevation, and vergence. A. Comparison of the three components (lateral version - *left*, elevation – *middle*, vergence – *right*) of predicted and true eye positions in a random subset of trials sampled from individual monkeys (rows 1-3) and all human subjects (combined, last row) at the moment when the target is turned OFF. **B.** The time-course of the above three components of eye movements during a random subset of trials from monkeys and humans. Blue and red dots denote the times at which the target was turned OFF and the end of movement, respectively. **C.** The empirically estimated cumulative density functions of the distribution over the subjects' lateral version (*left*), elevation (*middle*), and vergence (*right*) at the moment when the target was turned OFF (*blue*) and at the end of movement (*red*). Shaded regions denote standard errors obtained by bootstrapping. For each components, we used a bootstrap test with 10,000 bootstrap samples to determine whether parameters of the distributions estimated at the two time points were different. Specifically, we expect the magnitude of lateral version to approach zero over time (**Fig S2E**), so we tested whether the inter-quartile range (a measure of dispersion) was significantly smaller at the end of movement. On the other hand, we qualitatively expect the *magnitude* of elevation to increase over time (**Fig S2E**), so we tested whether the magnitude of the median was significantly greater at the end of movement. Finally, we qualitatively expect the vergence to increase over time (*i.e.* convergence, **Fig S2E**), so we tested whether the magnitude of the median was significantly greater at the end of movement. Asterisks denote significant difference ($p<0.001$) and n.s. denotes not significant according to the bootstrap test described above (*i.e.* whenever $p >= 0.001$). **D.** Time-course of the Pearson's correlation between the predicted and observed values of version (*left*), elevation (*middle*) and vergence (*right*) computed by aligning trials with respect to both the time when the target was turned OFF (denoted by the y-axis on the left) as well as the end of movement (denoted by the y-axis on the right). For humans, we pooled trials from all five subjects for the analysis shown here.

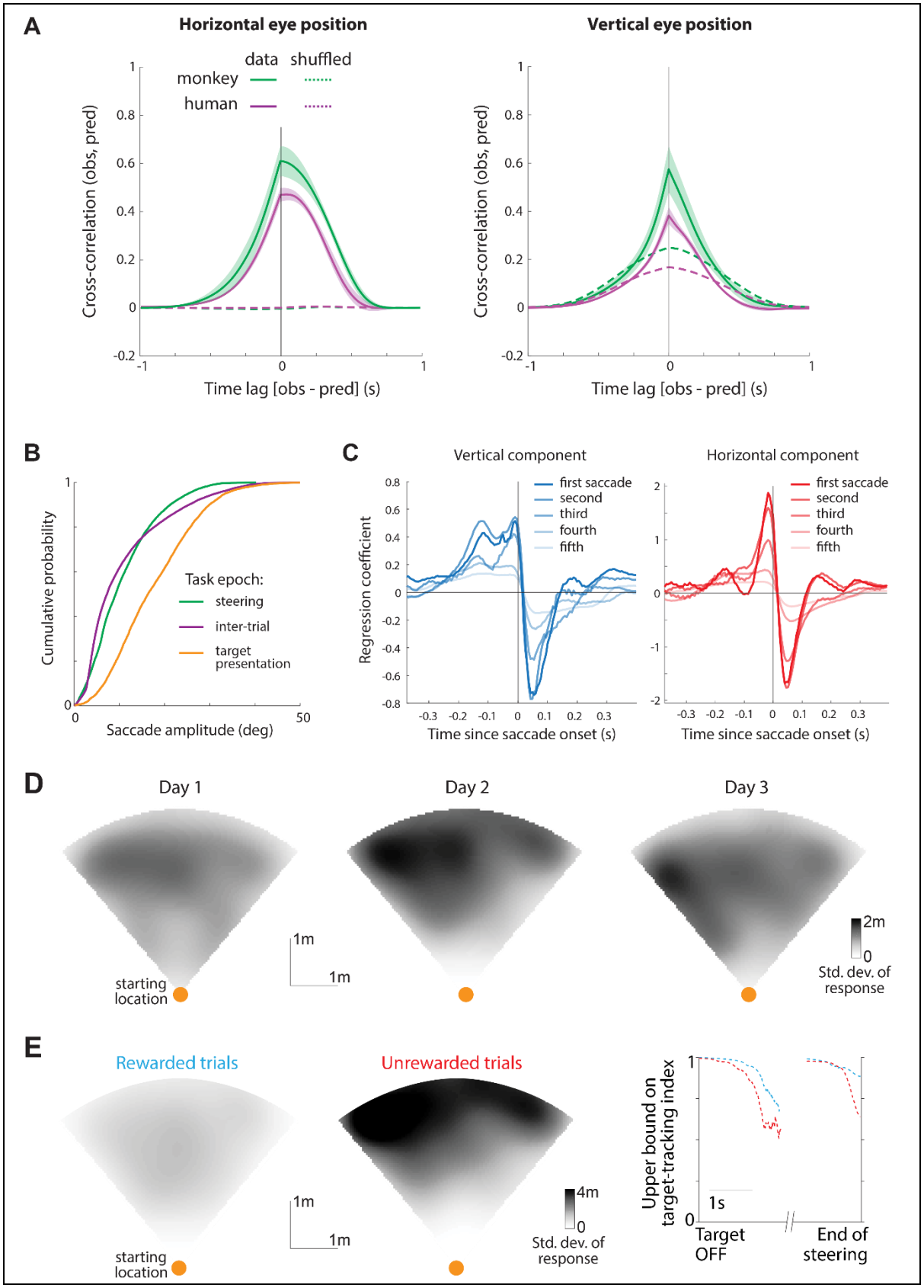
A
Horizontal eye position
Vertical eye position
data
shuffled
monkey
human
Cross-correlation (obs, pred)
Time lag [obs - pred] (s)
B
Cumulative probability
Task epoch:
steering
inter-trial
target presentation
Saccade amplitude (deg)
C
Vertical component
Horizontal component
first saccade
second
third
fourth
fifth
Regression coefficient
Time since saccade onset (s)
D
Day 1
Day 2
Day 3
starting location
1m
1m
2m
0
Std. dev. of response
E
Rewarded trials
Unrewarded trials
starting location
1m
1m
4m
0
Std. dev. of response
Upper bound on target-tracking index
1s
Target OFF
End of steering

Figure S4. [Panel **A**: Related to **Figure 2,** Panel **B-C**: Related to **Figure 3,** Panel **D-E**: Related to **Figure 4**]

Eye movements are not predictive of future target location. A. *Left*: Cross-correlogram between observed and predicted horizontal eye position computed by concatenating all the trials. Error bars denote ± 1 standard error in mean across subjects. A peak at positive (negative) time lag would correspond to observations lagging behind (leading) the predictions. *Right*: Cross-correlogram between observed and predicted vertical eye position. The time interval containing lower-bound of the 95% confidence interval (CI) of the peak cross-correlation did not exclude zero for both horizontal (monkeys: $\tau_{\text{peak}} = [-0.05\,, 0.15]$s ; humans: $\tau_{\text{peak}} = [-0.03\,, 0.2]$s) and vertical (monkeys: $\tau_{\text{peak}} = [-0.02\,, 0.04]$s, humans: $\tau_{\text{peak}} = [-0.03\,, 0.04]$s) components.

Saccadic eye movements in humans. B. Empirical cumulative distribution function of saccade amplitudes conditioned on the task epoch, averaged across all human subjects. Mean saccade amplitude ± SE: inter-trial – 10.8 ± 1.5°, target-presentation – 17.6 ± 2.2°, task phase – 10.4 ± 1.8°) **C.** The time-course of coefficients obtained by linearly regressing the amplitudes of the vertical (left) and horizontal (right) components of saccades (made while steering towards the target) against the corresponding components of the target tracking error (**Methods**). Regression was carried out separately for the first, second, third, fourth, and fifth saccades made during steering. Peak-to-peak difference in weights for vertical component: first saccade – 1.1 ± 0.3, fifth – 0.3 ± 0.1; horizontal component: first saccade – 3.6 ± 0.5, fifth – 0.5 ± 0.2.

Position uncertainty varied across days and across trials. D. Aerial view of the spatial map showing the standard deviation of stopping positions as a function of target location across trials from three different sessions of one monkey. The shape of the map is due to the restricted angles and distances at which targets could appear ($\pm 40°$ up to 4m away). Orange dot denotes starting location. **E.** Aerial view of the spatial map showing the standard deviation of stopping positions as a function of target location across a random subset of rewarded (*left*) and unrewarded (*middle*) trials of one monkey. *Right*: Time-course of the upper bound of the target-tracking index (**equation 3**) computed separately for the two sets of trials (blue – rewarded, red - unrewarded).

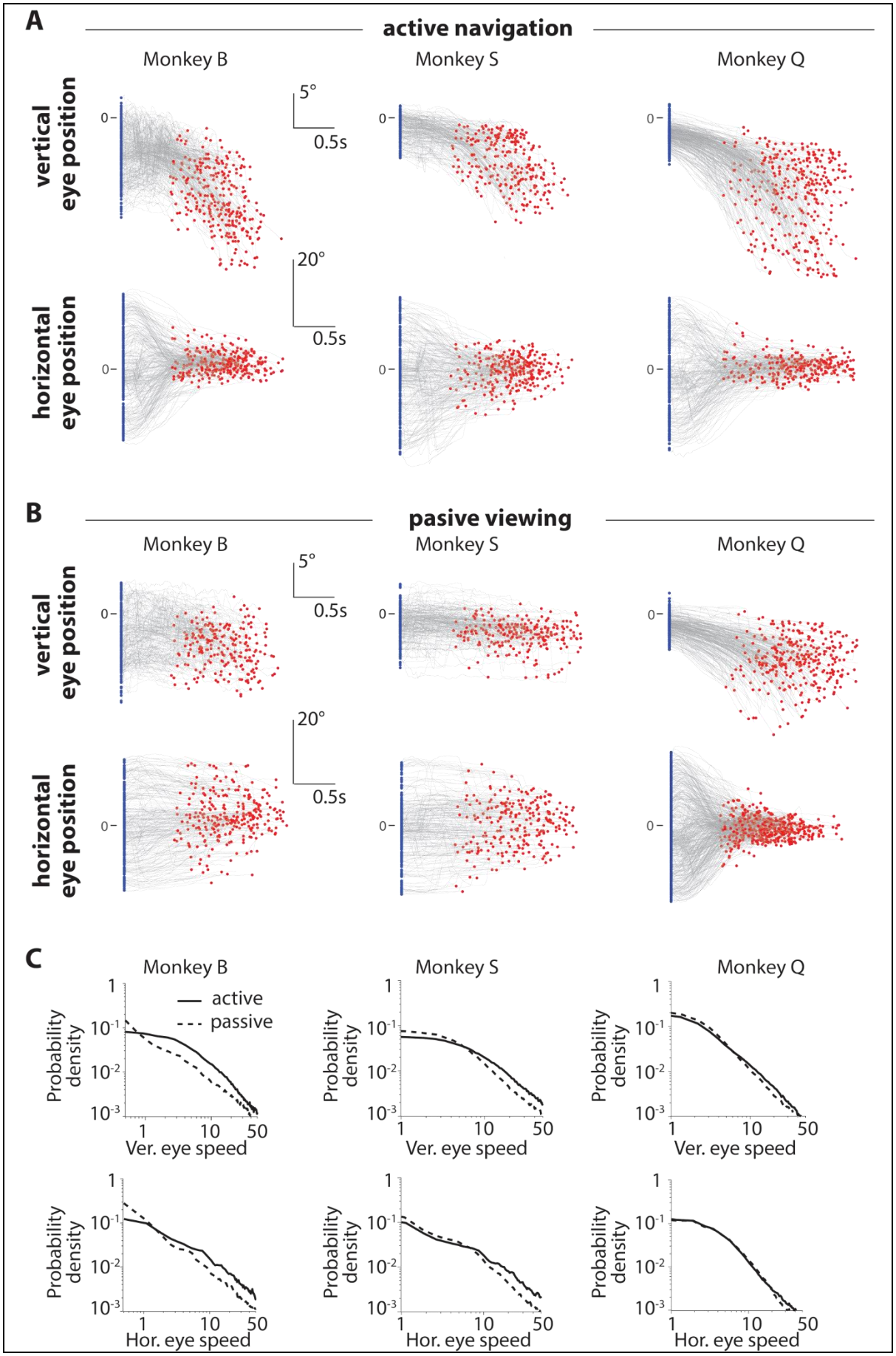
A
active navigation
Monkey B
Monkey S
Monkey Q
vertical eye position
horizontal eye position
5°
0.5s
20°
0.5s
0
B
pasive viewing
Monkey B
Monkey S
Monkey Q
vertical eye position
horizontal eye position
5°
0.5s
20°
0.5s
0
C
Monkey B
Monkey S
Monkey Q
active
passive
Probability density
1
10-1
10-2
10-3
1
10
50
Ver. eye speed
Hor. eye speed

Figure S5. [Related to **Figure 5**]

Temporal dynamics of eye position during active navigation and passive viewing (replay) blocks. A. The time-course of elevation (top) and lateral version (bottom) during a random subset of trials from a normal block of experiment (*active navigation block*). Blue and red dots denote the times at which the target was turned OFF and the end of movement, respectively. **B.** Similar to A, but data collected during a block of trials when the movie of the visual stimulus generated during the original task was replayed to the monkeys, with joystick control withheld (*passive viewing block*). During the passive block, eye movements of monkey B and monkey S do not resemble those observed during the normal experiment. **C.** Probability distribution over vertical (top) and horizontal (bottom) eye speeds under active navigation (*solid black*) and passive viewing (*dashed black*) conditions. Note that this is a log–log plot. Median vertical eye speed: active block – $6.3 \pm 2.8\ ^\circ/s$; passive block – $3.9 \pm 2.7\ ^\circ/s$. Median horizontal eye speed: active block – $5.7 \pm 2.3\ ^\circ/s$; passive block – $2.8 \pm 1.3\ ^\circ/s$.

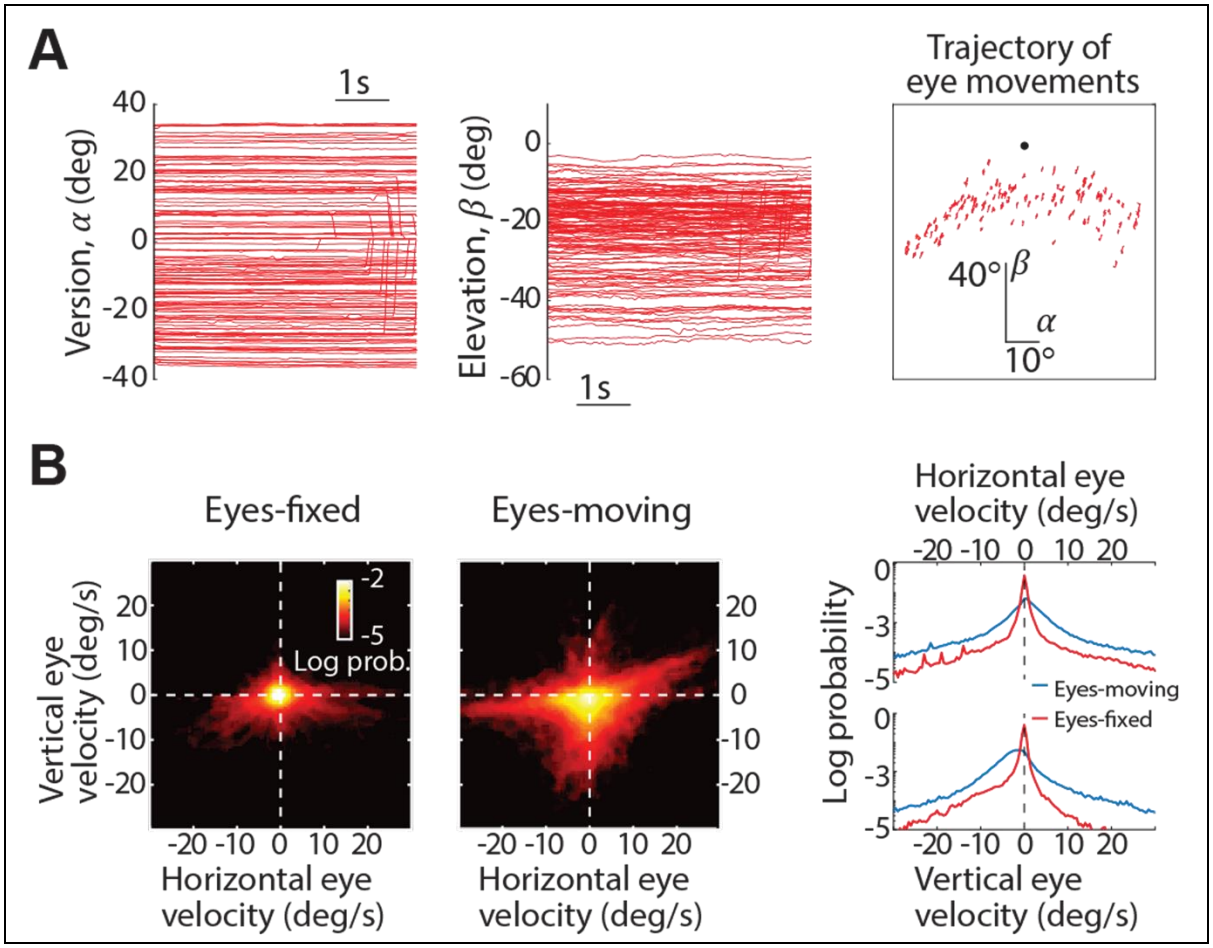

Figure S6. [Related to **Figure 6**]

Eye movements during the fixation task. A. Time-course of lateral version, α (left) and elevation, β (middle) of one human subject during a subset of trials in the 'Eyes-fixed' condition. The rightmost panel shows the trajectory (time-course) of eye movements in the α-β space during the same set of trials. Black dot denotes the origin $(\alpha, \beta) = (0,0)$. For this subject, the mean (± std) temporal variability (quantified as standard deviation σ of eye position across time, see **Methods**) of eye movements during the 'Eyes-fixed' condition was $0.5° \pm 0.3°$. See **Fig 5A** for summary data of all subjects. **B.** *Left*: The joint probability density of the distribution over the subjects' horizontal and vertical eye velocity, averaged across all human subjects, separately for trials from 'Eyes-fixed' and 'Eyes-moving' conditions. *Right*: Marginal distributions over horizontal and vertical eye velocity under the same two conditions. Note the much larger concentration of values around zero velocity during the 'Eyes-fixed' condition implying that subjects did not move their eyes during this condition.